ACS APPLIED MATERIALS & INTERFACES

Research Article

www.acsami.org

Expanded Porphyrins as Two-Dimensional Porous Membranes for CO_2 Separation

Ziqi Tian,[†] Sheng Dai,[‡,§] and De-en Jiang*[,†]

[†]Department of Chemistry, University of California, Riverside, California 92521, United States

[‡]Chemical Sciences Division, Oak Ridge National Laboratory, Oak Ridge, Tennessee 37831-6201, United States

[§]Department of Chemistry, The University of Tennessee, Knoxville, Tennessee 37996-1600, United States

Supporting Information

ABSTRACT: Porphyrin-based two-dimensional polymers have uniform micropores and close to atom-thin thicknesses, but they have not been explored for gas separation. Herein we design various expanded porphyrin derivatives for their potential application in membrane gas separation, using CO_2/N_2 as an example. Pore sizes are determined based on both van der Waals radii and electron density distribution. Potential energy curves for CO_2 and N_2 passing through are mapped by dispersion-corrected density functional theory calculations. The passing-through barriers are used to evaluate CO_2/N_2 separation selectivity. Promising subunits for CO_2 separation have been selected from the selectivity estimates. 2D membranes composed of amethyrin derivatives are shown to have high ideal selectivity on the order of 10^6 for CO_2/N_2 separation. Classical molecular dynamics simulation yields a permeance of 10^4−10^5 GPU for CO_2 through extended 2D membranes based on amethyrin derivatives. This work demonstrates that porphyrin systems could offer an attractive bottom-up approach for 2D porous membranes.

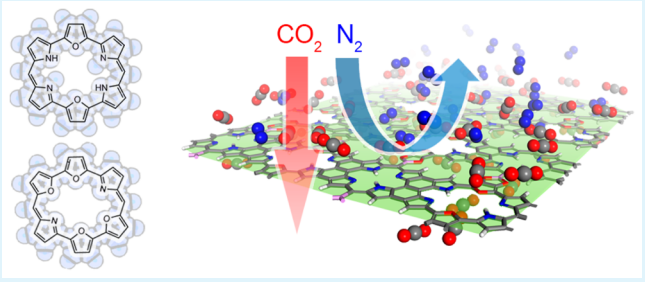

KEYWORDS: *gas separation, CO_2 capture, 2-dimensional polymer, ultrathin membrane, dispersion-corrected DFT*

1. INTRODUCTION

Burning fossil fuel generates a huge amount of CO_2, which contributes significantly to global warming. Separation of CO_2 from flue gas, or postcombustion carbon capture, plays a critical role in CO_2 emission reduction. Sorbent-based separation methods have used liquid amines,[1,2] ionic liquids,[3−5] metal−organic frameworks,[6,7] covalent−organic frameworks,[8,9] porous carbons,[10] and porous organic polymers.[11,12] However, regeneration of sorbents at higher temperatures to desorb CO_2 is energetically costly.

Membrane-based gas separation offers an attractive alternative, due to their small footprint and high energy-efficiency.[13,14] The productivity of membranes is measured by their gas permeance which is inversely proportional to the membrane thickness. Hence, ultrathin membranes with proper pore sizes and functional groups have the potential to offer both high selectivity and permeance.[15−18] Nanoporous graphene and graphene oxide have been studied experimentally and theoretically as molecule-sieving membranes.[19−25] However, it is difficult to introduce uniform and tunable micropores into graphene through a top-down approach. Recently, various two-dimensional (2D) polymers based on covalent organic frameworks (COFs) have been synthesized, providing a new possibility to construct membranes with uniform pores from the bottom up.[8,26−29]

Porphyrin derivatives are common building blocks for 2D polymeric constructions. Recently, porphyrin-based porous materials have been investigated for CO_2 capture.[30−33] Because of their high chemical stability, porphyrin units have been used to synthesize porous organic polymers (POPs) and metal−organic frameworks (MOFs). Bhaumik and co-workers synthesized porphyrin-based POPs and showed that they can have high BET surface areas and excellent CO_2 uptake (~19 wt% at 273 K and 1 bar).[30] Ma and co-workers made metal−organic materials from custom-designed porphyrin building blocks and found that they have permanent micropores and selective CO_2 uptake.[31] Zhang and co-workers reported direct X-ray observation of CO_2 inside a porphrinic MOF.[32] However, a 2D porous framework based on porphyrins has not been demonstrated experimentally.

Basic porphyrins are composed of four pyrrole rings. Expanded porphyrins[34−36] can have more than four heterocycles, resulting in a micropore in the center of the molecule. It is well-known that the center of porphyrins and expanded porphyrins can coordinate with metal cations or anions selectively in biochemistry and host−guest chemistry. Some derivatives have been used for selective anion extraction.[37] The nitrogen and oxygen groups around the rim of the center pore are Lewis bases and can serve as CO_2-phillic groups.

Received: April 15, 2015
Accepted: May 19, 2015
Published: May 19, 2015

DOI: 10.1021/acsami.5b03275
ACS Appl. Mater. Interfaces 2015, 7, 13073−13079

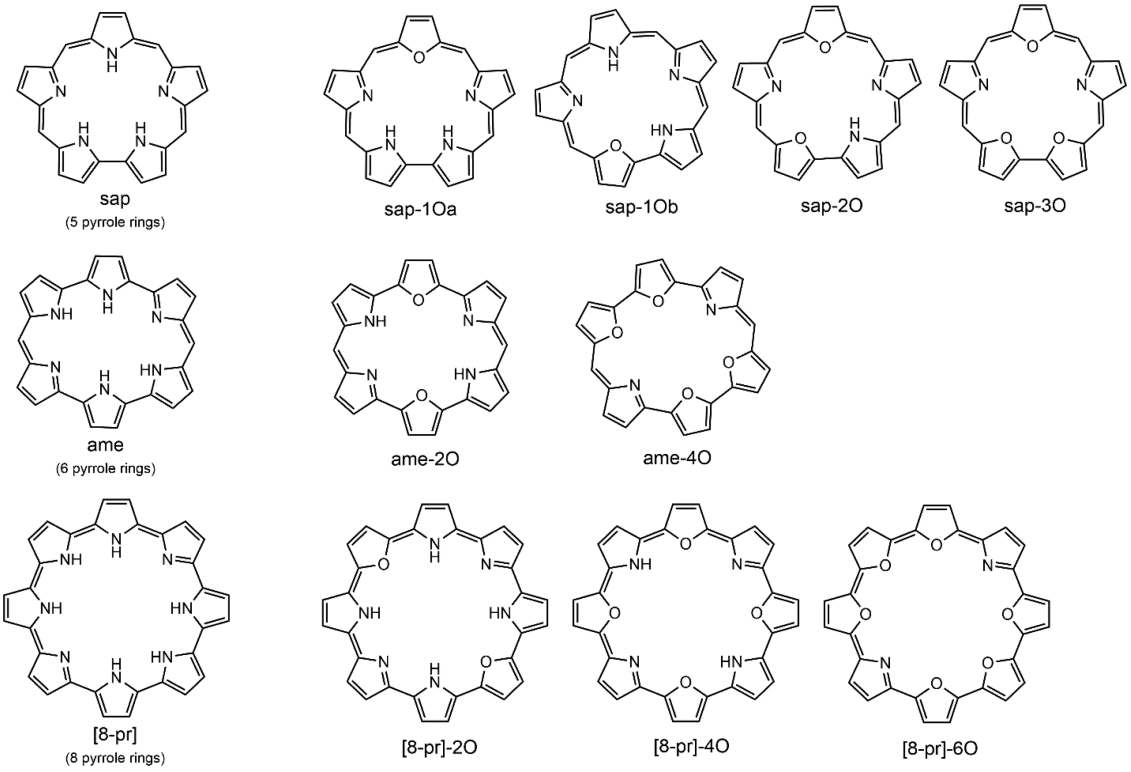

Figure 1. Proposed expanded porphyrins with large pores.

Hence the 2D nature of porphyrin derivatives and the functional N and O groups could offer high performance for CO_2 separation if they have appropriate pore sizes and are assembled into an extended membrane.

In this work, a series of expanded porphyrin derivatives are computationally designed. Their center pore sizes are evaluated from van der Waals radii and electron density distribution. Potential energy curves for CO_2 and N_2 passing through the center pores are computed from density functional theory to estimate ideal selectivity. Then two extended 2D membranes are constructed from the most promising porphyrin building blocks; the performance of such membranes is then simulated by classical molecular dynamics.

2. CALCULATION DETAILS

Geometry relaxation of the porphyrin building blocks was performed with the Gaussian 09 program package[38] at the M06-2*x*/6-31+G(d) level.[39,40] Frequency calculations were performed at the same level to confirm that all the obtained structures were local minima with no imaginary frequency. On the basis of these optimized geometries, iso-electron density surfaces were plotted at different iso-values to determine pore sizes of the porphyrins. Furthermore, natural bond orbital (NBO)[41] calculations were employed to analyze partial charges on atoms.

B-LYP calculations[42,43] with DFT-D3[44] correction in the Turbomole V6.5 electronic structure package[45] were used to explore potential energy curves of a single CO_2 or N_2 molecule crossing the pore center of selected expanded porphyrins. Def2-QZVPP orbital and auxiliary basis sets were utilized. It was reported that dispersion interactions could be reproduced quite well at this level, with a mean absolute deviation of 1 kcal/mol compared with the CCSD(T)/CBS results.[46] The gas molecule approached the pore center with the molecular axis perpendicular to the porphyrin plane. Geometries of porphyrin molecules were fixed.

To simulate gas permeation through an extended membrane, classical molecular dynamics simulations were performed with the LAMMPS software package[47] in the NVT ensemble. The Nose-Hoover thermostat was applied to keep gas temperature at 300 K. 2D periodic boundary conditions in the *xy* directions were employed. The atoms in the membrane were fixed. Their atomic charges were obtained from ESP fitting at the B3LYP/6-31G(d) level. Models with three partial charges were adopted for CO_2 and N_2 molecules.[48] van der Waals parameters were fitted according to calculated potential energy curves for atoms in gas molecules and around pores in porphyrins (see Table S1 and Table S2 in the Supporting Information for these parameters). The cutoff distance of intermolecular interaction was 12.0 Å. The dimension of the membrane model was 38.54 Å × 47.27 Å. Six parallel dynamic simulations for 50 ns were performed. Coordinates for both the molecular porphyrin models and the extended systems were provided in the Supporting Information.

Table 1. Pore Sizes of Various Porphyrin Derivatives

	$d_{vdW\text{-}cor}$/Å	d_{el}/Å (isovalue/a.u.)	
		(0.001)	(0.002)
sap	0.79	0.88	1.30
sap-1Oa	1.26	1.31	1.75
sap-1Ob	0.94	1.14	1.68
sap-2O	1.38	1.38	1.89
sap-3O	2.05	1.79	2.37
ame	0.94	0.72	1.02
ame-2O	1.18	1.49	1.81
ame-4O	2.14	1.82	2.32
[8-pr]	3.48	3.25	3.57
[8-pr]-2O	3.24	3.11	3.45
[8-pr]-4O	3.33	3.10	3.47
[8-pr]-6O	3.92	3.07	3.36
CO_2	3.24	3.54	3.30
N_2	3.43	3.62	3.36

DOI: 10.1021/acsami.5b03275
ACS Appl. Mater. Interfaces 2015, 7, 13073−13079

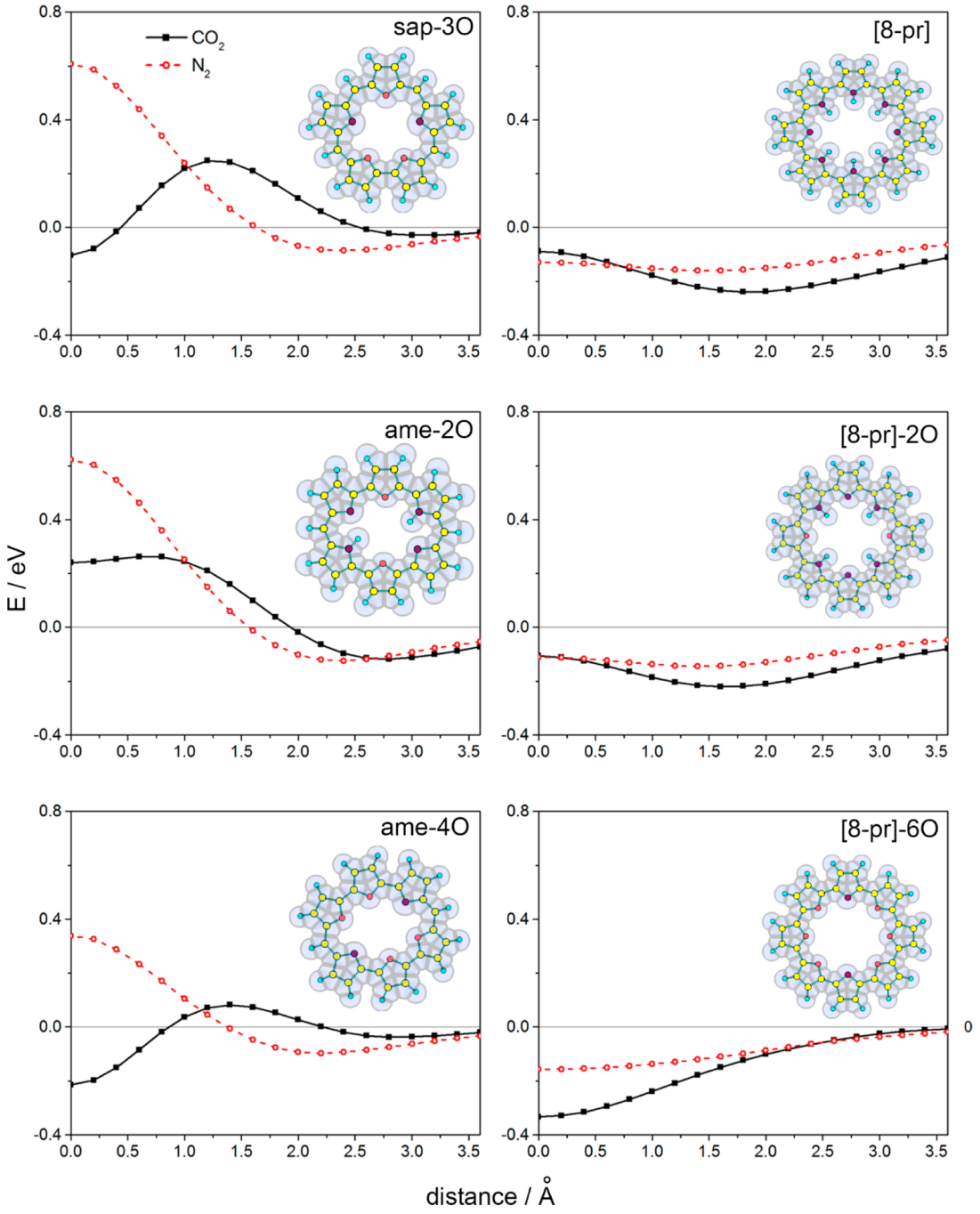

Figure 2. Potential energy curves for CO_2 and N_2 interacting with selected porous porphyrins at the B-LYP-D3/def2-QZVPP level. Distance is from the center-of-mass of the gas molecule to the center of the pore.

3. RESULTS AND DISCUSSION

3.1. Geometry and Pore Size. In many biochemical compounds, there are divalent metal cations in the center of porphyrins, such as Fe^{2+} in heme, Mg^{2+} in chlorophyll, and Zn^{2+} in protoporphyrin, indicating that the pore radius of the normal porphyrin anion is about 0.8 Å. This pore is too small for any gas molecule to pass though. Hence, we focus on expanded porphyrins with larger pores. Three classes of expanded porphyrin derivatives are investigated, named as sapphyrin, amethyrin, and cyclo[8]pyrrole following the literature convention.[36] They are composed of 5, 6, and 8 pyrrole subunits, respectively, and denoted as sap, ame, and [8-pr] for short in the following discussion. For neutral porphyrin derivatives, some nitrogen atoms in pyrrole subunits are hydrogenated. These hydrogen atoms hinder gas molecule diffusion through the center pore. To enlarge the center pores, pyrrole rings are alternatively substituted by furans or pyridines to eliminate hydrogen atoms in the pore. Geometry relaxations with DFT calculations show that pyridine replacement leads to corrugated structure and nonplanar geometry, because of steric hindrance between the 2- and 6- hydrogens of pyridine. In comparison, furan substitutions keep the structures planar. We will focus on the furan-substituted expanded porphyrins, as shown in Figure 1.

The simplest way to determine pore diameters is to directly measure the smallest distance between two opposite atoms

DOI: 10.1021/acsami.5b03275
ACS Appl. Mater. Interfaces 2015, 7, 13073−13079

surrounding the pore and to take into account van der Waals radii of H, N, and O.[49] The results are $d_{vdW\text{-}cor}$ in Table 1. One can see that the pores of all the sapphyrin and amethyrin derivatives may be too small for either CO_2 or N_2 to pass through, while the pore sizes of [8-pr]-2O and [8-pr]-4O should be just right for CO_2 permeation. One can also determine pore sizes by the electron-density iso-value surface, which is called d_{el} in Table 1. Of course, d_{el} is dependent on the predetermined electron density iso-value. Our previous work[50] has shown that diameters of common gas molecules obtained from iso-electronic density surfaces at relatively small iso-values (0.001, 0.0015, and 0.002 au) are in good agreement with kinetic diameters in references.[51] We find that the pore diameters estimated at iso-values of 0.001 are similar to the corresponding $d_{vdW\text{-}cor}$ values (Table 1).

Given that the diameter of CO_2 is only slightly smaller than that of N_2, the pore size alone may not offer enough selectivity. One also needs to consider the functional groups around the pore rim. Previously, it has been shown that factors including heteroatom-containing polar groups, dipole−quadrupole, acid−base, and other weak interactions between CO_2 and the absorbents can significantly improve CO_2 affinity.[52,53] The nitrogen and oxygen heteroatoms around the micropore in the centers of porphyrins are Lewis bases and may offer stronger interaction with CO_2 than N_2. To probe such interaction, we need to examine the potential energy surfaces of CO_2 and N_2 passing through the porphyrin pore.

3.2. Potential Energy Surface and Ideal Selectivity. Potential energy curves for CO_2 and N_2 interacting with porphyrin derivatives, such as sap-3O, ame-2O, ame-4O, [8-pr], [8-pr]-2O, and [8-pr]-6O, are mapped to obtain the barriers for gas passing-through (Figure 2). Although CO_2 is a nonpolar molecule, the C atom has a positive charge (1.055 |e|) and the two O atoms have a negative charge (−0.527 |e|), leading to a large quadrupole moment which can interact with the charges on N and O atoms in porphyrins (at −0.48 |e| and −0.43 ± 0.03 |e|, respectively). The potential energy curves show that sap-3O, ame-2O, and ame-4O can distinguish CO_2 from N_2. Energy barriers for CO_2 passing through sap-3O, ame-2O, and ame-4O (ΔE_{CO2} in Table 2) are 0.352, 0.381, and 0.297 eV, respectively; for sap-3O and ame-4O, the barrier is for CO_2 escaping from the pore, rather than getting into the pore, because escaping from the pore is the rate-limiting step. On the other hand, there are almost no energy barriers for both CO_2 and N_2 going into the pores of [8-pr] derivatives, indicating that the pores will not offer enough selectivity for CO_2 over N_2.

On the basis of the energy barriers, we can estimate the ideal CO_2/N_2 selectivity of the porphyrin derivatives by the Arrhenius equation.[19] Table 2 shows that sap-3O, ame-2O, and ame-4O have a large enough difference between CO_2 passing-through barrier (ΔE_{CO2}) and N_2 passing-through barrier (ΔE_{N2}). Assuming that the passing-through processes of both gases follow the Arrhenius rate equation with the same pre-exponential factors, we obtained ideal selectivity $S_{CO2/N2} = e^{-\Delta\Delta E/RT}$, in which $\Delta\Delta E = \Delta E_{CO2} - \Delta E_{N2}$. High selectivities ranging from 10^2 to 10^6 indicate the potential of ame-2O, ame-4O, and sap-3O as building blocks for 2D porous organic membranes. These high CO_2/N_2 selectivites result from both the surface basicity (nitrogen- and oxygen-containing groups) on the 2D porous membranes consisting of porphyrin building blocks and the right pore sizes. To confirm the high selectivity and to estimate the permeance, we constructed extended 2D membranes based on the ame-2O and ame-4O building blocks.

Table 2. Gas Passing-through Barriers and Ideal CO_2/N_2 Selectivies of Selected Porous Porphyrins

	sap-3O	ame-2O	ame-4O
ΔE_{CO2}/eV	0.352	0.381	0.297
ΔE_{N2}/eV	0.694	0.747	0.436
$\Delta\Delta E$/eV	0.342	0.366	0.139
selectivity (300 K)	5.6×10^5	1.4×10^6	2.2×10^2

3.3. Construction of a 2D Membrane. Table 2 shows that both sap-3O and ame derivatives have high ideal CO_2/N_2 selectivities. From a practical point of view, ame-2O and ame-4O are more promising for 2-D construction because of their

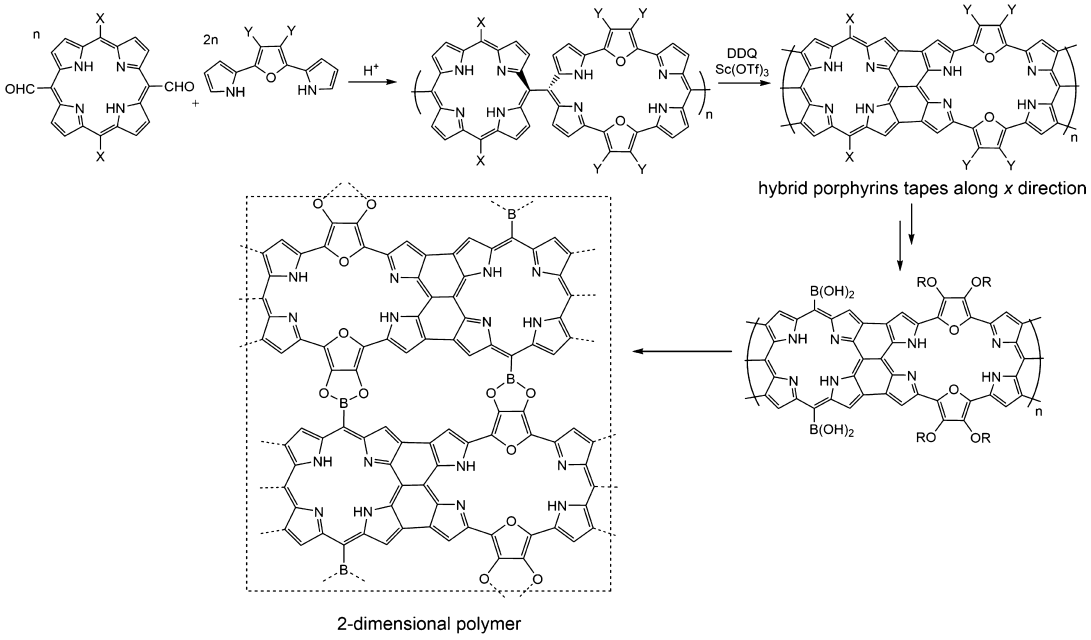

Figure 3. Proposed synthetic route toward a 2D membrane structure based on ame-2O.

DOI: 10.1021/acsami.5b03275
ACS Appl. Mater. Interfaces 2015, 7, 13073−13079

high symmetries in comparison with sap-3O. Ame derivatives have been obtained experimentally.[54] Some meso−meso linked porphyrin−hexaphyrin hybrid tapes have also been synthesized,[55] providing a potential path to obtain ultrathin membranes with appropriate micropores based on porphyrin building blocks. Moreover, a strategy for covalent linking of building blocks by sequential binding of specific sites was demonstrated,[56] leading to improved polymerization quality. As an example, we constructed a 2D polyporphyrin system based on the ame-2O building block. Hybrid porphyrins tapes can grow along the *x* direction at first and then connect with each other by B−O bonds or other groups in the *y* direction. Figure 3 shows the proposed synthetic route for this 2D system.

Figure 4 shows the extended structures of the 2D porous membranes based on ame-2O and ame-4O units. To test their performance for CO_2/N_2 separation, we set up a bichamber system to simulate CO_2/N_2 passing through our proposed porphyrin-based membranes. The upper chamber is pressurized with gases, while the lower chamber is started with vacuum (Figure 5a). Then classical MD simulations are run to follow the gas permeation. Figure 5b shows that no N_2 molecules pass through the ame-2O or ame-4O membrane, while about 25 CO_2 molecules permeate into the other side of the ame-4O membrane within the 50 ns time frame, confirming its high separation selectivity. The CO_2 permeation rate of the ame-2O membrane is about 1 order of magnitude smaller than that of the ame-4O membrane. Numbers of permeated CO_2 are almost linear with time. From the rates, we derived a permeance of 8.0×10^3 GPU (1 GPU = 3.35×10^{-10} mol m^{-2} s^{-1} Pa^{-1}) for the ame-2O membrane and 7.2×10^4 GPU for the ame-4O membrane. Figure 5c shows a snapshot of CO_2 passing through the ame-2O membrane.

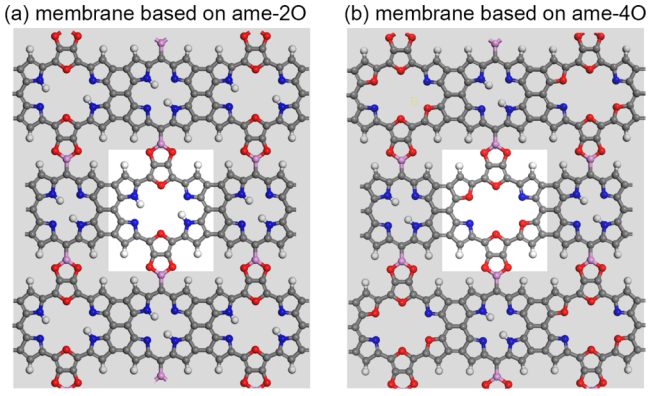

Figure 4. Extended 2D membrane structure based on ame-2O (a) and ame-4O (b). Color code: C, gray; H, white; O, red; N, blue; B, pink.

3.4. Comparison with Previous Studies and Implications. Schrier[21,57] and Liu[22,25,58] et al. have previously studied porous two-dimensional polymer and nitrogen-doping graphene by classical molecular dynamics simulations. They obtained CO_2 permeances on the order of magnitude of 10^5 GPU. In their models, the pore sizes were approximately 3−4 Å. The permeance we obtained for the ame-4O membrane is close to their values. The pore size of the ame-2O is smaller, leading to a small simulated permeance (~10^4 GPU). The high CO_2/N_2 selectivity for the porphyrin-based 2D membranes coupled with high permeance could offer a potential approach to overcome the Robeson upperbound.[59] When discussing the cost analysis of carbon capture, Merkel et al. reported that CO_2 permeances exceeding 4000 GPU with a CO_2/N_2 selectivity at 40 corresponds to a cost of CO_2 capture at below $15/ton CO_2.[60] In consideration of the excellent selectivity for CO_2/N_2 separation with a high permeance of 10^4 GPU for CO_2, the proposed expanded porphyrin-based membrane would have good performance for postcombustion CO_2 capture.

4. CONCLUSIONS

In summary, we have designed a series of expanded porphyrin derivatives as building blocks for 2D porous membranes.

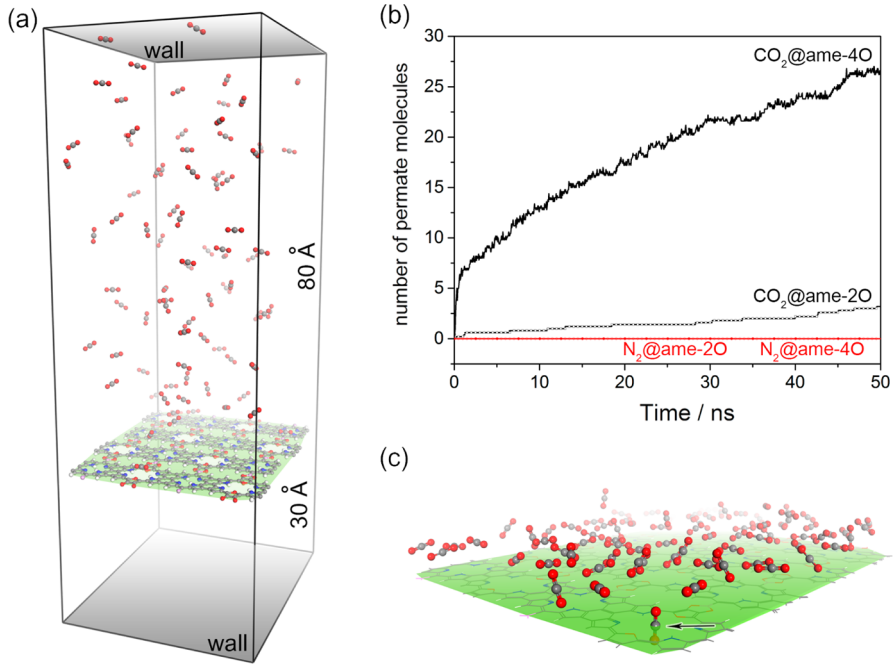

Figure 5. (a) A bichamber setup for molecular dynamic simulation. (b) Pure-gas permeation through the ame-2O and ame-4O based membranes at an initial pressure of 20 atm. (c) Snapshot of CO_2 passing through the ame-2O membrane.

DOI: 10.1021/acsami.5b03275
ACS Appl. Mater. Interfaces 2015, 7, 13073−13079

On the basis of potential energy curves of CO_2 and N_2 passing through the center pores, sap-3O, ame-2O, and ame-4O were considered promising for separating CO_2 from N_2. Ame-2O and ame-4O, which are composed of 6 five-membered heterocycles, have CO_2/N_2 selectivities on the order of 10^6 and 10^2, respectively, estimated from energy barriers of gas passing-through. The basic groups on the 2D porous membranes and the appropriate pore sizes result in the high selectivity for CO_2/N_2 separation. 2D extended membranes were constructed with the ame-2O and ame-4O building blocks. Molecular dynamic simulations confirmed that the high CO_2/N_2 selectivity for these membranes with a CO_2 permeance of on the order of 10^4 to 10^5 GPU. Therefore, expanded porphyrins could be potentially used as building blocks to make 2D porous membranes for gas separation.

■ ASSOCIATED CONTENT

Supporting Information

Optimized geometries of porphyrin building blocks, geometries of porphyrin-based 2D-sheet models, and force field parameters (partial charges and van der Waals parameters) for atoms in gas molecules and around micropores. The Supporting Information is available free of charge on the ACS Publications website at DOI: 10.1021/acsami.5b03275.

■ AUTHOR INFORMATION

Corresponding Author

*E-mail: de-en.jiang@ucr.edu. Phone: +1-951-827-4430.

Notes

The authors declare no competing financial interest.

■ ACKNOWLEDGMENTS

This work was supported by the Division of Chemical Sciences, Geosciences and Biosciences, Office of Basic Energy Sciences, U.S. Department of Energy. This research used resources of the National Energy Research Scientific Computing Center, a DOE Office of Science User Facility supported by the Office of Science of the U.S. Department of Energy under Contract No. DE-AC02-05CH11231.

■ REFERENCES

(1) Dumée, L.; Scholes, C.; Stevens, G.; Kentish, S. Purification of Aqueous Amine Solvents Used in Post Combustion CO_2 Capture: A Review. *Int. J. Greenhouse Gas Control* **2012**, *10*, 443−455.

(2) Gouedard, C.; Picq, D.; Launay, F.; Carrette, P. L. Amine Degradation in CO_2 Capture. I. A Review. *Int. J. Greenhouse Gas Control* **2012**, *10*, 244−270.

(3) Hasib-ur-Rahman, M.; Siaj, M.; Larachi, F. Ionic Liquids for CO_2 Capture-Development and Progress. *Chem. Eng. Process.* **2010**, *49*, 313−322.

(4) Ramdin, M.; de Loos, T. W.; Vlugt, T. J. H. State-of-the-Art of CO_2 Capture with Ionic Liquids. *Ind. Eng. Chem. Res.* **2012**, *51*, 8149−8177.

(5) Zhang, X.; Zhang, X.; Dong, H.; Zhao, Z.; Zhang, S.; Huang, Y. Carbon Capture with Ionic Liquids: Overview and Progress. *Energy Environ. Sci.* **2012**, *5*, 6668−6681.

(6) Sabouni, R.; Kazemian, H.; Rohani, S. Carbon Dioxide Capturing Technologies: A Review Focusing on Metal Organic Framework Materials (MOFs). *Environ. Sci. Pollut. Res.* **2014**, *21*, 5427−5449.

(7) Pimentel, B. R.; Parulkar, A.; Zhou, E. K.; Brunelli, N. A.; Lively, R. P. Zeolitic Imidazolate Frameworks: Next-Generation Materials for Energy-Efficient Gas Separations. *ChemSusChem* **2014**, *7*, 3202−3240.

(8) Furukawa, H.; Yaghi, O. M. Storage of Hydrogen, Methane, and Carbon Dioxide in Highly Porous Covalent Organic Frameworks for Clean Energy Applications. *J. Am. Chem. Soc.* **2009**, *131*, 8875−8883.

(9) Dawson, R.; Cooper, A. I.; Adams, D. J. Nanoporous Organic Polymer Networks. *Prog. Polym. Sci.* **2012**, *37*, 530−563.

(10) Dutta, S.; Bhaumik, A.; Wu, K. C. W. Hierarchically Porous Carbon Derived from Polymers and Biomass: Effect of Interconnected Pores on Energy Applications. *Energy Environ. Sci.* **2014**, *7*, 3574−3592.

(11) Li, P. Z.; Zhao, Y. L. Nitrogen-Rich Porous Adsorbents for CO_2 Capture and Storage. *Chem.-Asian J.* **2013**, *8*, 1680−1691.

(12) Xu, C.; Hedin, N. Microporous Adsorbents for CO_2 Capture - A Case for Microporous Polymers? *Mater. Today* **2014**, *17*, 397−403.

(13) Freemantle, M. Membranes for Gas Separation. *Chem. Eng. News* **2005**, *83*, 55.

(14) Gin, D. L.; Noble, R. D. Designing the Next Generation of Chemical Separation Membranes. *Science* **2011**, *332*, 674−676.

(15) Carta, M.; Malpass-Evans, R.; Croad, M.; Rogan, Y.; Jansen, J. C.; Bernardo, P.; Bazzarelli, F.; McKeown, N. B. An Efficient Polymer Molecular Sieve for Membrane Gas Separations. *Science* **2013**, *339*, 303−307.

(16) Zhu, X.; Tian, C. C.; Chai, S. H.; Nelson, K.; Han, K. S.; Hagaman, E. W.; Veith, G. M.; Mahurin, S. M.; Liu, H. L.; Dai, S. New Tricks for Old Molecules: Development and Application of Porous N-doped, Carbonaceous Membranes for CO_2 Separation. *Adv. Mater.* **2013**, *25*, 4152−4158.

(17) Peng, Y.; Li, Y. S.; Ban, Y. J.; Jin, H.; Jiao, W. M.; Liu, X. L.; Yang, W. S. Metal-Organic Framework Nanosheets as Building Blocks for Molecular Sieving Membranes. *Science* **2014**, *346*, 1356−1359.

(18) Guo, H.; Zhang, W.; Lu, N.; Zhuo, Z.; Zeng, X. C.; Wu, X.; Yang, J. CO_2 Capture on h-BN Sheet with High Selectivity Controlled by External Electric Field. *J. Phys. Chem. C* **2015**, *119*, 6912−6917.

(19) Jiang, D. E.; Cooper, V. R.; Dai, S. Porous Graphene as the Ultimate Membrane for Gas Separation. *Nano Lett.* **2009**, *9*, 4019−4024.

(20) Blankenburg, S.; Bieri, M.; Fasel, R.; Mullen, K.; Pignedoli, C. A.; Passerone, D. Porous Graphene as an Atmospheric Nanofilter. *Small* **2010**, *6*, 2266−2271.

(21) Schrier, J. Fluorinated and Nanoporous Graphene Materials As Sorbents for Gas Separations. *ACS Appl. Mater. Interfaces* **2011**, *3*, 4451−4458.

(22) Liu, H. J.; Cooper, V. R.; Dai, S.; Jiang, D. E. Windowed Carbon Nanotubes for Efficient CO_2 Removal from Natural Gas. *J. Phys. Chem. Lett.* **2012**, *3*, 3343−3347.

(23) Kim, H. W.; Yoon, H. W.; Yoon, S. M.; Yoo, B. M.; Ahn, B. K.; Cho, Y. H.; Shin, H. J.; Yang, H.; Paik, U.; Kwon, S.; Choi, J. Y.; Park, H. B. Selective Gas Transport Through Few-Layered Graphene and Graphene Oxide Membranes. *Science* **2013**, *342*, 91−95.

(24) Joshi, R. K.; Carbone, P.; Wang, F. C.; Kravets, V. G.; Su, Y.; Grigorieva, I. V.; Wu, H. A.; Geim, A. K.; Nair, R. R. Precise and Ultrafast Molecular Sieving Through Graphene Oxide Membranes. *Science* **2014**, *343*, 752−754.

(25) Liu, H.; Chen, Z.; Dai, S.; Jiang, D.-e. Selectivity Trend of Gas Separation through Nanoporous Graphene. *J. Solid State Chem.* **2015**, *224*, 2−6.

(26) Cote, A. P.; Benin, A. I.; Ockwig, N. W.; O'Keeffe, M.; Matzger, A. J.; Yaghi, O. M. Porous, Crystalline, Covalent Organic Frameworks. *Science* **2005**, *310*, 1166−1170.

(27) Spitler, E. L.; Dichtel, W. R. Lewis Acid-Catalysed Formation of Two-Dimensional Phthalocyanine Covalent Organic Frameworks. *Nat. Chem.* **2010**, *2*, 672−677.

(28) Feng, X.; Ding, X.; Jiang, D. Covalent Organic Frameworks. *Chem. Soc. Rev.* **2012**, *41*, 6010−6022.

(29) Colson, J. W.; Dichtel, W. R. Rationally Synthesized Two-Dimensional Polymers. *Nat. Chem.* **2013**, *5*, 453−465.

(30) Modak, A.; Nandi, M.; Mondal, J.; Bhaumik, A. Porphyrin Based Porous Organic Polymers: Novel Synthetic Strategy and Exceptionally High CO_2 Adsorption Capacity. *Chem. Commun.* **2012**, *48*, 248−250.

(31) Wang, X.-S.; Chrzanowski, M.; Gao, W.-Y.; Wojtas, L.; Chen, Y.-S.; Zaworotko, M. J.; Ma, S. Vertex-Directed Self-Assembly of a High Symmetry Supermolecular Building Block Using a Custom-Designed Porphyrin. *Chem. Sci.* **2012**, *3*, 2823−2827.
(32) Johnson, J. A.; Chen, S.; Reeson, T. C.; Chen, Y. S.; Zeng, X. C.; Zhang, J. Direct X-Ray Observation of Trapped CO_2 in a Predesigned Porphyrinic Metal-Organic Framework. *Chem.—Eur. J.* **2014**, *20*, 7632−7637.
(33) Modak, A.; Pramanik, M.; Inagaki, S.; Bhaumik, A. A Triazine Functionalized Porous Organic Polymer: Excellent CO_2 Storage Material and Support for Designing Pd Nanocatalyst for C−C Cross-Coupling Reactions. *J. Mater. Chem. A* **2014**, *2*, 11642−11650.
(34) Jasat, A.; Dolphin, D. Expanded Porphyrins and Their Heterologs. *Chem. Rev.* **1997**, *97*, 2267−2340.
(35) Osuka, A.; Saito, S. Expanded Porphyrins and Aromaticity. *Chem. Commun.* **2011**, *47*, 4330−4339.
(36) Saito, S.; Osuka, A. Expanded Porphyrins: Intriguing Structures, Electronic Properties, and Reactivities. *Angew. Chem., Int. Ed.* **2011**, *50*, 4342−4373.
(37) Seidel, D.; Lynch, V.; Sessler, J. L. Cyclo[8]Pyrrole: A Simple-to-Make Expanded Porphyrin with No Meso Bridges. *Angew. Chem., Int. Ed.* **2002**, *41*, 1422−1425.
(38) Frisch, M. J.; Trucks, G. W.; Schlegel, H. B.; Scuseria, G. E.; Robb, M. A.; Cheeseman, J. R.; Scalmani, G.; Barone, V.; Mennucci, B.; Petersson, G. A.; Nakatsuji, H.; Caricato, M.; Li, X.; Hratchian, H. P.; Izmaylov, A. F.; Bloino, J.; Zheng, G.; Sonnenberg, J. L.; Hada, M.; Ehara, M.; Toyota, K.; Fukuda, R.; Hasegawa, J.; Ishida, M.; Nakajima, T.; Honda, Y.; Kitao, O.; Nakai, H.; Vreven, T.; Montgomery, J. A.; Peralta, Jr., J. E.; Ogliaro, F.; Bearpark, M.; Heyd, J. J.; Brothers, E.; Kudin, K. N.; Staroverov, V. N.; Keith, T.; Kobayashi, R.; Normand, J.; Raghavachari, K.; Rendell, A.; Burant, J. C.; Iyengar, S. S.; Tomasi, J.; Cossi, M.; Rega, N.; Millam, J. M.; Klene, M.; Knox, J. E.; Cross, J. B.; Bakken, V.; Adamo, C.; Jaramillo, J.; Gomperts, R.; Stratmann, R. E.; Yazyev, O.; Austin, A. J.; Cammi, R.; Pomelli, C.; Ochterski, J. W.; Martin, R. L.; Morokuma, K.; Zakrzewski, V. G.; Voth, G. A.; Salvador, P.; Dannenberg, J. J.; Dapprich, S.; Daniels, A. D.; Farkas, O.; Foresman, J. B.; Ortiz, J. V.; Cioslowski, J.; Fox, D. J.. *Gaussian 09*, Revision D.01; Gaussian, Inc.: Wallingford, CT, 2009.
(39) Zhao, Y.; Truhlar, D. G. The M06 Suite of Density Functionals for Main Group Thermochemistry, Thermochemical Kinetics, Noncovalent Interactions, Excited States, and Transition Elements: Two New Functionals and Systematic Testing of Four M06-Class Functionals and 12 Other Functionals. *Theor. Chem. Acc.* **2008**, *120*, 215−241.
(40) Zhao, Y.; Truhlar, D. G. Density Functionals with Broad Applicability in Chemistry. *Acc. Chem. Res.* **2008**, *41*, 157−167.
(41) Glendening, E. D.; Reed, A. E.; Carpenter, J. E.; Weinhold, F. *NBO*, version 3.1; University of Wisconsin: Madison, 1998.
(42) Becke, A. D. Density-Functional Exchange-Energy Approximation with Correct Asymptotic-Behavior. *Phys. Rev. A* **1988**, *38*, 3098−3100.
(43) Lee, C. T.; Yang, W. T.; Parr, R. G. Development of the Colle-Salvetti Correlation-Energy Formula into a Functional of the Electron-Density. *Phys. Rev. B* **1988**, *37*, 785−789.
(44) Grimme, S.; Antony, J.; Ehrlich, S.; Krieg, H. A Consistent and Accurate ab initio Parametrization of Density Functional Dispersion Correction (DFT-D) for the 94 Elements H-Pu. *J. Chem. Phys.* **2010**, *132*, 154104(1)−154104(19).
(45) Ahlrichs, R.; Bar, M.; Haser, M.; Horn, H.; Kolmel, C. Electronic-Structure Calculations on Workstation Computers - the Program System Turbomole. *Chem. Phys. Lett.* **1989**, *162*, 165−169.
(46) Goerigk, L.; Grimme, S. A Thorough Benchmark of Density Functional Methods for General Main Group Thermochemistry, Kinetics, and Noncovalent Interactions. *Phys. Chem. Chem. Phys.* **2011**, *13*, 6670−6688.
(47) Plimpton, S. Fast Parallel Algorithms for Short-Range Molecular-Dynamics. *J. Comput. Phys.* **1995**, *117*, 1−19.
(48) Vrabec, J.; Stoll, J.; Hasse, H. A Set of Molecular Models for Symmetric Quadrupolar Fluids. *J. Phys. Chem. B* **2001**, *105*, 12126−12133.
(49) Rowland, R. S.; Taylor, R. Intermolecular Nonbonded Contact Distances in Organic Crystal Structures: Comparison with Distances Expected from van der Waals Radii. *J. Phys. Chem.* **1996**, *100*, 7384−7391.
(50) Mehio, N.; Dai, S.; Jiang, D. E. Quantum Mechanical Basis for Kinetic Diameters of Small Gaseous Molecules. *J. Phys. Chem. A* **2014**, *118*, 1150−1154.
(51) Breck, D. W. *Zeolite Molecular Sieve: Structure, Chemistry and Use*; John Wiley & Sons, Inc.: New York, 1974.
(52) Hao, G. P.; Li, W. C.; Qian, D.; Lu, A. H. Rapid Synthesis of Nitrogen-Doped Porous Carbon Monolith for CO_2 Capture. *Adv. Mater.* **2010**, *22*, 853−857.
(53) Sevilla, M.; Valle-Vigón, P.; Fuertes, A. B. N-Doped Polypyrrole-Based Porous Carbons for CO_2 Capture. *Adv. Funct. Mater.* **2011**, *21*, 2781−2787.
(54) Sessler, J. L.; Weghorn, S. J.; Hiseada, Y.; Lynch, V. Hexaalkyl Terpyrrole - a New Building-Block for the Preparation of Expanded Porphyrins. *Chem.—Eur. J.* **1995**, *1*, 56−67.
(55) Mori, H.; Tanaka, T.; Lee, S.; Lim, J. M.; Kim, D.; Osuka, A. meso-meso Linked Porphyrin-[26]Hexaphyrin-Porphyrin Hybrid Arrays and Their Triply Linked Tapes Exhibiting Strong Absorption Bands in the NIR Region. *J. Am. Chem. Soc.* **2015**, *137*, 2097−2106.
(56) Lafferentz, L.; Eberhardt, V.; Dri, C.; Africh, C.; Comelli, G.; Esch, F.; Hecht, S.; Grill, L. Controlling On-Surface Polymerization by Hierarchical and Substrate-Directed Growth. *Nat. Chem.* **2012**, *4*, 215−220.
(57) Schrier, J. Carbon Dioxide Separation with a Two-Dimensional Polymer Membrane. *ACS Appl. Mater. Interfaces* **2012**, *4*, 3745−3752.
(58) Liu, H. J.; Dai, S.; Jiang, D. E. Insights into CO_2/N_2 Separation through Nanoporous Graphene from Molecular Dynamics. *Nanoscale* **2013**, *5*, 9984−9987.
(59) Robeson, L. M. The Upper Bound Revisited. *J. Membr. Sci.* **2008**, *320*, 390−400.
(60) Merkel, T. C.; Lin, H. Q.; Wei, X. T.; Baker, R. Power Plant Post-Combustion Carbon Dioxide Capture: an Opportunity for Membranes. *J. Membr. Sci.* **2010**, *359*, 126−139.

DOI: 10.1021/acsami.5b03275
ACS Appl. Mater. Interfaces 2015, 7, 13073−13079